A Heterogeneous Palladium Catalyst for the Polymerization of Olefins Prepared by Halide Abstraction Using Surface R 3 Si + Species

Jiaxin Gao, Rick Dorn, Guillaume P. Laurent, Frédéric Perras, Aaron Rossini, Matthew Conley

To cite this version:

Jiaxin Gao, Rick Dorn, Guillaume P. Laurent, Frédéric Perras, Aaron Rossini, et al.. A Heterogeneous Palladium Catalyst for the Polymerization of Olefins Prepared by Halide Abstraction Using Surface R 3 Si + Species. Angewandte Chemie International Edition, 2022, 61 (20), pp.e202117279. 10.1002/anie.202117279. hal-03905712

HAL Id: hal-03905712
https://hal.sorbonne-universite.fr/hal-03905712

Submitted on 12 May 2023

A Journal of the Gesellschaft Deutscher Chemiker
Angewandte Chemie
GDCh
International Edition
www.angewandte.org

Title: A Heterogeneous Palladium Catalyst for the Polymerization of Olefins Prepared by Halide Abstraction Using Surface R3Si + Species

Authors: Jiaxin Gao, Rick W. Dorn, Guillaume P. Laurent, Frédéric A. Perras, Aaron J. Rossini, and Matthew Conley

To be cited as: *Angew. Chem. Int. Ed.* **2022**, e202117279

Link to VoR: https://doi.org/10.1002/anie.202117279

WILEY-VCH

10.1002/anie.202117279

A Heterogeneous Palladium Catalyst for the Polymerization of Olefins Prepared by Halide Abstraction Using Surface R_3Si^+ Species

Jiaxin Gao,[a] Rick W. Dorn,[b,c] Guillaume P. Laurent,[c,d] Frédéric A. Perras,[c] Aaron J. Rossini,[b,c] and Matthew P. Conley[a]*

[a] J. Gao, Prof. Dr. M. P. Conley
Department of chemistry
University of California, Riverside
Riverside, CA, 92521, USA
E-mail: matthew.conley@ucr.edu

[b] R. W. Dorn, Prof. Dr. A. J. Rossini
Department of Chemistry
Iowa State University,
Ames, Iowa 50011, United States

[c] R. W. Dorn, G. P. Laurent, F. A. Perras, Prof. Dr. A. J. Rossini
U.S. Department of Energy
Ames Laboratory
Ames, Iowa 50011, United States

[d] G. P. Laurent
CNRS, Laboratoire de Chimie de la Matière Condensée de Paris
Sorbonne Université,
LCMCP, F-75005 Paris, France

Supporting information for this article is given via a link at the end of the document

Abstract: The silylium-like surface species [^{i}Pr$_3$Si][(R^{F}O)$_3$Al–OSi≡)] activates (N^N)Pd(CH$_3$)Cl (N^N = Ar-N=CMeMeC=N-Ar, Ar = 2,6-*bis*(diphenylmethyl)-4-methylbenzene) by chloride ion abstraction to form [(N^N)Pd–CH$_3$][(R^{F}O)$_3$Al–OSi≡)] (**1**). A combination of FTIR, solid-state NMR spectroscopy, and reactions with CO or vinyl chloride establish that **1** shows similar reactivity patterns as (N^N)Pd(CH$_3$)Cl activated with Na[B(Ar^F)$_4$]. Multinuclear $^{13}C\{^{27}Al\}$ RESPDOR and $^1H\{^{19}F\}$ S-REDOR experiments show that the (N^N)Pd–CH$_3^+$ fragment is weakly coordinated to the [(R^{F}O)$_3$Al–OSi≡)] anion, indicating that the palladium fragment interacts with a siloxane bridge on silica. **1** catalyzes the polymerization of ethylene with similar activities as [(N^N)Pd–CH$_3$]$^+$ in solution and incorporates up to 0.4 % methyl acrylate in copolymerization reactions. **1** produces polymers with significantly higher molecular weight than the solution catalyst, and generates the highest molecular weight polymers currently reported in copolymerization reactions of ethylene and methylacrylate.

Introduction

Heterogeneous catalysts produce the vast majority of polyolefin materials.[1] The work-flow to generate an active heterogeneous catalyst for olefin polymerization usually involves activation of a Group 4 metal pre-catalyst with a large excess of alkylaluminum[2] or partially hydrolyzed alkylaluminum[3] in the presence of a high surface area oxide.[4] These mixtures can evolve into well-defined surface species that produce narrow molecular weight distributions of polyolefin.[5] Ni- or Pd-catalysts for olefin polymerization incorporate monomers containing heteroatoms,[6] but are generally incompatible with this heterogeneous work-flow. A small family of (α-diimine)NiBr$_2$ pre-catalysts are active in the presence of alkylaluminum activators and SiO$_2$ or MgCl$_2$, but produce broad molecular weight polymers; incorporation of polar monomers was not reported.[7] Similar compositions are not suitable for Pd catalysts because alkylaluminum reagents abstract bidentate nitrogen ligands from the metal.[8]

Examples of heterogeneous Pd catalysts for olefin polymerization are shown in Figure 1a. Phosphine-sulfonate Pd

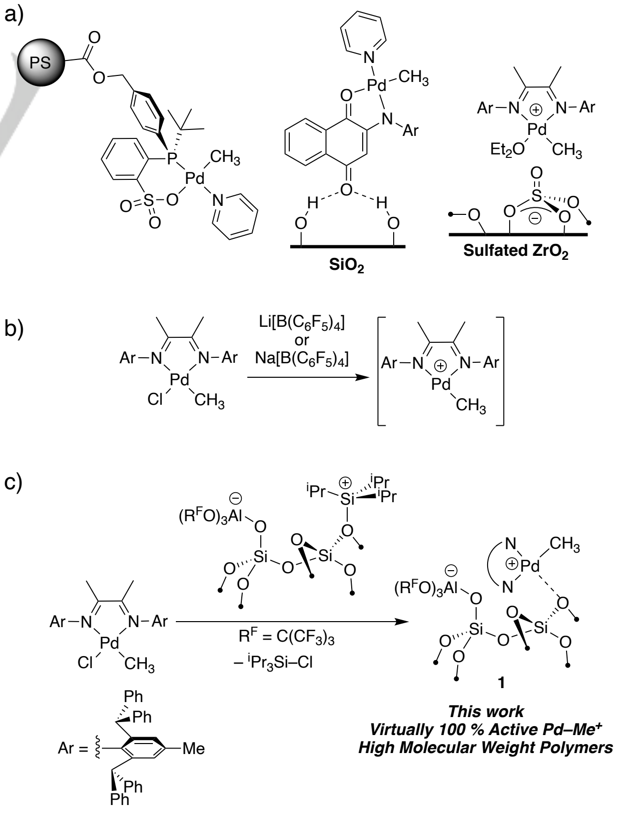

Figure 1. Examples of heterogeneous Pd-catalysts for olefin polymerization (a); Halide abstraction reactivity common in homogeneous polymerization reactions with (α-diimine)Pd–catalysts (b); application of a surface-bound silylium-like ion in halide abstraction to generate heterogeneous [(α-diimine)Pd–CH_3]$^+$ (c).

complexes supported on functionalized polystyrene beads are active in polymerization reactions, but have lower activities and yield polymers with lower molecular weights than homogeneous analogs.[9] Anilinonapthoquinone Pd-complexes adsorb onto silica by forming hydrogen bonds between surface silanols and the distal carbonyl of the functionalized quinone ligand. The distribution of Pd sites copolymerize ethylene and methylacrylate to form polymers with broad molecular weight distributions ($Đ = M_w/M_n = 3.9$).[10] Heterogeneous derivatives of Brookhart's [(α-diimine)Pd–CH_3]$^+$ catalyst[6c] are available from the reaction of (α-diimine)Pd(CH_3)$_2$ with sulfated zirconium oxide, an established weakly coordinating support,[11] to form palladium sites that produce narrow molecular weight distributions of polymers ($Đ$ = 1.4 – 1.9), though only ~9 % of the Pd sites are active from ^{2}H labelling studies.[12] The origin of the low active site count is unclear, but the grafting reaction generates more methane than expected suggesting that some Pd sites lack a Pd–CH_3 group required to polymerize olefins.

The most common method to generate active (α-diimine)Pd–CH_3^+ is halide abstraction using Li[B(C_6F_5)$_4$] or Na[B(C_6F_5)$_4$] from (α-diimine)Pd(CH_3)Cl, Figure 1b. Integrating similar salts onto an oxide support is challenging and currently limited to reactions of neutral Lewis acids with silica that form surface species that are unreactive in halide abstraction reactions.[13] We recently reported examples of silylium-like (R_3Si^+) species supported on Lewis acid activated silica ([^{i}Pr$_3$Si][(R^FO)$_3$Al–OSi≡)]).[14] Silylium-like ions are very strong Lewis acids[15] capable of abstracting halides from transition metal, lanthanide, or actinide complexes.[16] This paper describes the halide abstraction reactivity of [^{i}Pr$_3$Si][(R^FO)$_3$Al–OSi≡)] with (α-diimine)Pd(CH_3)Cl containing Ar-N=CMeMeC=N-Ar (Ar = 2,6-*bis*(diphenylmethyl)-4-methylbenzene, N^N, Figure 1c).[17] This reaction results in the formation of [(N^N)Pd–CH_3][(R^FO)$_3$Al–OSi≡)] that are active in olefin (co)polymerization reactions.

Results and Discussion

The reaction of [^{i}Pr$_3$Si][(R^FO)$_3$Al–OSi≡)] (~0.2 mmol R_3Si^+ g^{-1}) with (N^N)Pd(CH_3)Cl in C_6D_6 slurry at room temperature results in the formation of ^{i}Pr$_3$Si–Cl (0.054 ± 0.001 mmol g^{-1}) and [(N^N)Pd–CH_3][(R^FO)$_3$Al–OSi≡)] (**1**, Figure 1c). Prolonged reaction times do not increase the amount of ^{i}Pr$_3$Si–Cl formed in this reaction. The ^{29}Si cross-polarization magic angle spinning (CPMAS) NMR spectrum of **1** contain signals at 70 ppm from residual R_3Si^+ (Figure S5), indicating that some of the silylium sites in [^{i}Pr$_3$Si][(R^FO)$_3$Al–OSi≡)] are not reactive towards (N^N)Pd(CH_3)Cl. ICP-OES of **1** gives 0.048 ± 0.001 mmol Pd g^{-1}. This value is close to the amount of ^{i}Pr$_3$Si–Cl evolved in the formation of **1**, supporting the 1:1 reaction stoichiometry in the grafting shown in Figure 1c.

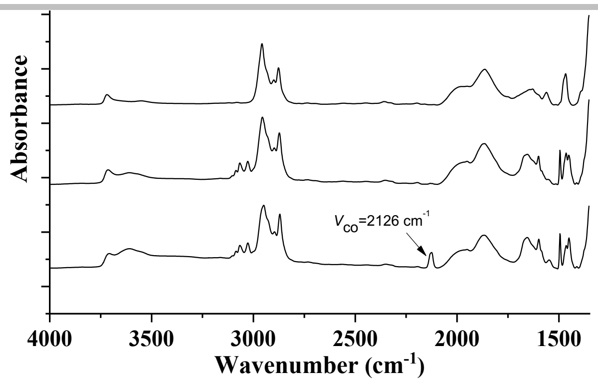

Figure 2. FTIR spectra of [^{i}Pr$_3$Si][(R^FO)$_3$AlOSi≡](top), **1** (middle), **1-CO** (bottom).

The FTIR spectrum of [^{i}Pr$_3$Si][(R^FO)$_3$Al–OSi≡)] and **1** are shown in Figure 2. The FTIR spectrum of [^{i}Pr$_3$Si][(R^FO)$_3$Al–OSi≡)] was previously reported,14 and contains C-H vibrations (ν_{CH} = 2958, 2899, 2877 cm^{-1}) and bends (ν_{CH} = 1465 and 1349 cm^{-1}) typical for *sp^3* carbons. **1** contains similar sp^3 C-H vibrations and bends that are assigned to unreacted ^{i}Pr$_3$Si$^+$ groups, but also contains *sp^2* C-H vibrations (ν_{CH} = 3027, 3066 cm^{-1}) as well as the vibrations for the C=N at 1655 cm^{-1} and aromatic C=C at 1599cm^{-1}.

Contacting **1** with excess CO at room temperature results in the formation of **1-CO** (eq 1). The FTIR of **1-CO** is also shown in Figure 2 (bottom spectrum) and contains a ν_{CO} stretch at 2126 cm^{-1}. This spectrum lacks an associated Pd-acyl $\nu_{C=O}$ stretch indicating that migratory insertion does not occur under these conditions. Similar behavior was observed for [(N^N)Pd(CH_3)CO][B(Ar^F)$_4$] generated in solution (ν_{CO} = 2129 cm^{-1}).[17b] This result indicates that the Pd center in **1** is in a similar electronic environment as [(N^N)Pd(CH_3)CO][B(Ar^F)$_4$] and that the [(R^FO)$_3$Al–OSi≡)] surface anion is weakly coordinated to the (N^N)Pd-CH_3^+ fragment in **1**.

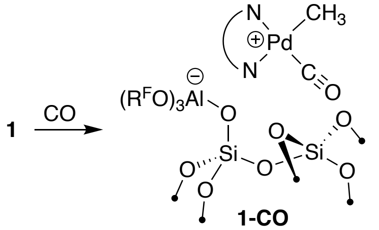

1-CO

(1)

The static ^{27}Al NMR spectrum of **1** is characteristic of the distorted tetrahedral environment expected for the [(R^FO)$_3$Al–OSi≡)] surface anion (Figure S5). The ^{13}C CPMAS spectrum of **1** contains signals for the α-diimine ligand at 141 (Ar), 129 (Ar), and 52 (*C*HAr$_2$) ppm (Figure S4). Signals at 19, 16 and 13 ppm are assigned to residual ^{i}Pr$_3$Si$^+$, methyl groups of the diimine ligand, and the Pd–CH_3^+. The reaction of (N^N)Pd($^{13}CH_3$)Cl with [^{i}Pr$_3$Si][(R^FO)$_3$Al–OSi≡)] generates **1-^{13}C**, and behaves similarly to the natural abundance reaction described above. The ^{13}C CPMAS NMR spectrum of **1-^{13}C** contains an intense signal at 16 ppm assigned to the Pd–Me$^+$ (Figure S4). This signal is 11 ppm higher in frequency than the (N^N)Pd($^{13}CH_3$)Cl signal in $CDCl_3$ solution, as expected for (N^N)Pd–CH_3^+.

^{13}C{^{27}Al} Phase-Modulated Resonance-Echo Saturation-Pulse Double-Resonance (PM-RESPDOR)[18] experiments of **1-^{13}C** contain minimal differences in spectra intensity for the aromatic carbons at long dipolar recoupling times (Figure S6), indicating that ^{13}C signals from (N^N)Pd-$^{13}CH_3^+$ sites are far (> ~5 Å) from the aluminum of the [(R^FO)$_3$Al–OSi≡)] surface anion, consistent with a weakly coordinating ion-pair.

The $^1H\{^{19}F\}$ Dipolar Heteronuclear Multiple Quantum Coherence (D-HMQC) NMR spectrum of **1** is shown in Figure 3. This spectrum contains background ^1H and ^{19}F NMR signals from the O-rings used to seal the rotor (†, Figure 3a, Figure S7), but the aromatic signals from **1** are well-resolved at ~ 7 ppm. Importantly, the broad aromatic ^1H NMR signal centered at 7ppm (*Ar*-N=CMeMeC=N-*Ar*) correlates with the ^{19}F NMR signal at –76 ppm from [(R^FO)$_3$Al–OSi≡)], showing that some of the hydrogens from the phenyl rings are close to the fluorine atoms of [(R^FO)$_3$Al–OSi≡)]. ^1H–^{19}F distance measurements to the aromatic ^1H sites were performed using the Symmetry-based Resonance-Echo Double-Resonance (S-REDOR) experiment;[19] the dephasing curve from this experiment is given in Figure 3b. The experimental $^1H\{^{19}F\}$ S-REDOR curve was fitted to a model that accounts for both the large number of unique ^1H-^{19}F distances and the multispin nature of the dephasing. This ultimately, reduces curve fitting to Pd-Al internuclear distance as a single parameter (see the Supporting Information for details). The best fit Pd-Al internuclear distance is 11 Å, indicating that the [(N^N)Pd–CH$_3$]$^+$ cation and the [(R^FO)$_3$Al–OSi≡] anion are proximate on the surface (Figure 3c). This data is also consistent with a weakly coordinating ion-pair, and suggests the [(N^N)Pd–CH$_3$]$^+$ fragment interacts with a nearby ≡Si–O–Si≡ bridge as shown in Figure 1c, which is common in supported organometallics.[20]

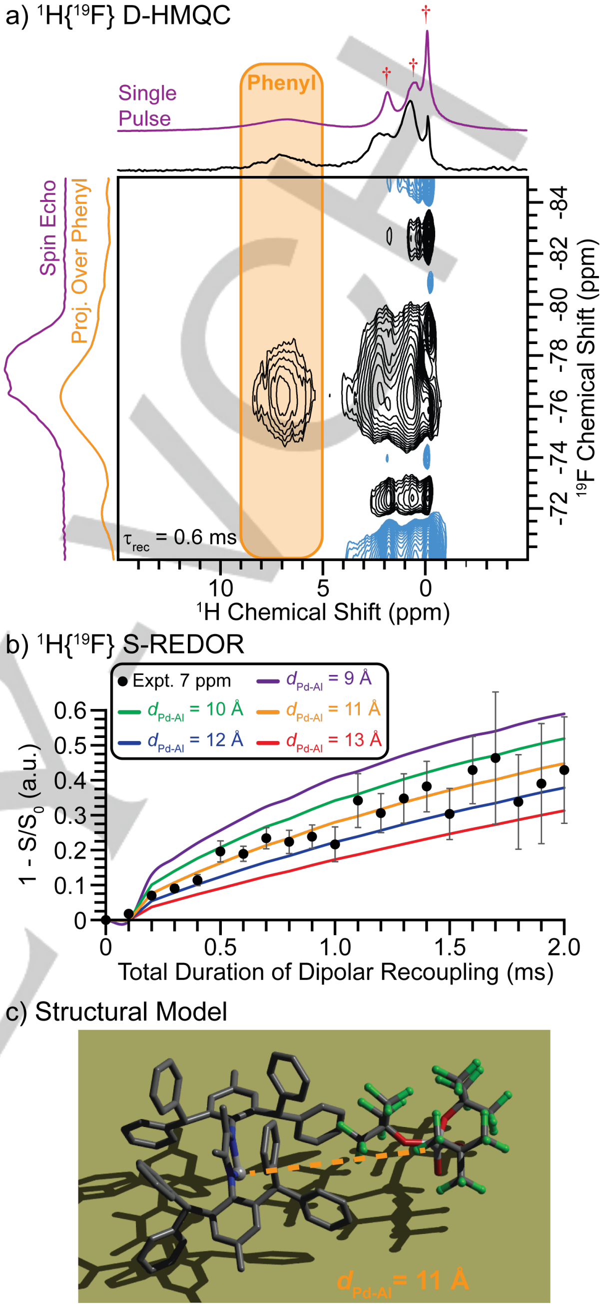

Figure 3. (a) 2D $^1H\{^{19}F\}$ D-HMQC NMR spectrum of **1** recorded with 0.6 ms of total $SR4_1^2$ heteronuclear dipolar recoupling applied to the ^1H spins. The highlighted region shows the ^1H NMR signals of the ^1H signals from the aromatic rings from the (N^N) ligand and the red daggers (†) are ^1H NMR signals from the O-rings from air-free inserts. The indirectly-detected ^{19}F spectrum is a projection over the ^1H NMR signals from the phenyl H atoms (denoted by the highlighted orange box). ^1H single-pulse and ^{19}F spin echo spectra are above the 2D projections. (b) $^1H\{^{19}F\}$ S-REDOR curve for the ^1H NMR signals centered at *ca.* 7 ppm. The black circles correspond to the experimental data points and the solid lines correspond to numerically simulated $^1H\{^{19}F\}$ S-REDOR curves with Pd-Al internuclear distances (d_{Pd-Al}) of 9 Å (purple), 10 Å (green), 11 Å (orange), 12 Å (blue), or 13 Å (red,). All spectra were recorded at B_0 = 9.4 T with 20 kHz MAS in a NMR probe cooled to –40 °C. (c) Structural model of **1** illustrating the spatial proximity of (N^N)Pd-CH$_3^+$ and the [(R^FO)$_3$Al-OSi≡] surface anion. H atoms are omitted for clarity.

10.1002/anie.202117279

Reactivity of 1 with Vinyl Chloride. In solution cationic Pd–Me$^+$ complexes react with vinyl chloride to generate Pd–Cl$^+$ that cannot insert olefins.[21] Therefore, reactions of **1** with vinyl chloride should result in the formation of [(N^N)Pd–Cl][(R^{F}O)$_3$Al–OSi≡)] (**2**) and propene, eq 2, and quantification of propene would correlate with the quantity of Pd–Me$^+$ in **1** capable of inserting an olefin. A similar method was used to quantify active Zr–H$^+$ sites in a ternary heterogeneous catalyst,[5] and is complementary to other quantification methods that involve contacting an active catalyst with an olefin that inhibits chain growth or quenching an active catalyst with a substrate containing a label.[22]

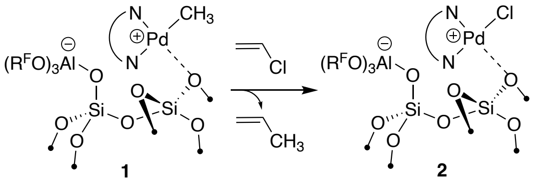

(2)

Contacting **1** or **1-^{13}C** with vinyl chloride (~100 equiv per Pd) and heating to 60 °C reproducibly results in the formation of 0.050 ± 0.003 mmol propene g^{-1}. This value is essentially identical to the Pd present in **1**, indicating that virtually all Pd–Me$^+$ sites in **1** are active in olefin insertion reactions. The methyl region of the ^{1}H NMR spectrum of the propene formed in the reaction of **1-^{13}C** with vinyl chloride is shown in Figure 4a, the full spectrum is provided in the Supporting Information (Figure S12). The coupling pattern indicates that 3-^{13}C-propene ($^1J_{CH}$ = 125.7 Hz, $^3J_{HH}$ = 6.5 Hz, $^4J_{HH}$ = 1.5 Hz) forms as the major product (78 %) of this reaction. Small amounts of 1-^{13}C-propene (22 % %; $^3J_{CH}$ = 4.8 Hz, $^3J_{HH}$ = 6.5 Hz, $^4J_{HH}$ = 1.5 Hz) also form in this reaction. Consistent with the formation of **2**, the ^{13}C CPMAS spectrum of **1** contacted with vinyl chloride lacks the signal assigned to the Pd–^{13}CH$_3^+$ group (Figure S11).

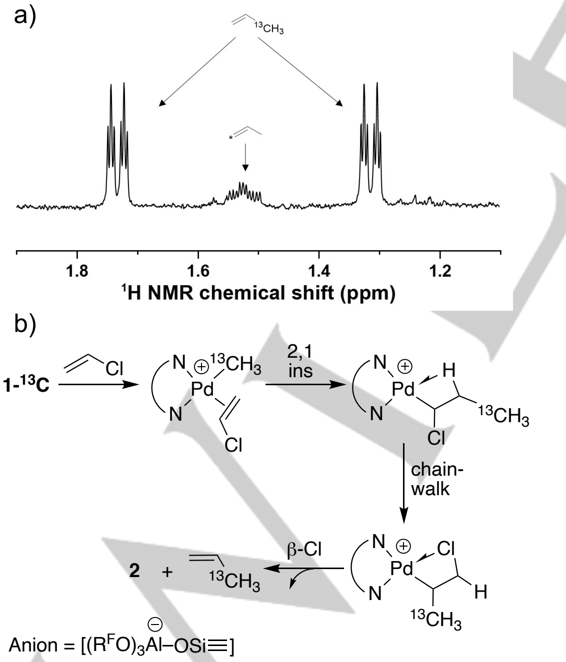

Figure 4. ^{1}H NMR spectrum from 1.1 – 1. 8 ppm showing methyl resonances from 3-^{13}C-propene (a). Proposed mechanism to form 3-^{13}C-propene from **1-^{13}C** and vinyl chloride (b).

The formation of 3-^{13}C-propene can be rationalized by the steps shown in Figure 4b. Cationic Pd–R$^+$ insert vinyl chloride by 2,1 insertion.[21b, 23] The unobserved β-H agostic Pd-alkyl chain-walks to give the β-chloro alkyl intermediate, which rapidly β-chloride eliminates to form [(N^N)Pd–Cl][(R^{F}O)$_3$Al–OSi≡)] and 3-^{13}C-propene. Control experiments show that 3-^{13}C-propene isomerizes to 1-^{13}C-propene in the presence of [^{i}Pr$_3$Si][(R^{F}O)$_3$Al–OSi≡)],[24] indicating that this product is a result of a side reaction with residual ^{i}Pr$_3$Si$^+$ sites present in **1**.

The polymerization activity of **1** as a function of temperature in cyclohexane under 150 psi ethylene pressure on demand is shown in Figure 5. Characterization data for the polymers are summarized in Table 1. Under these conditions **1** polymerizes ethylene at 20 °C to form 6.0 x 10^5 g$_{PE}$ mol$_{Pd}^{-1}$ h^{-1} of branched polyethylene (26 branches/1000C). This activity is close to homogeneous solutions of (N^N)PdMeCl activated with Na[B(Ar^F)$_4$] (5.8 x 10^5 g$_{PE}$ mol$_{Pd}^{-1}$ h^{-1}) with similar branch density in the polymer (25 branches/1000C).[17b] In contrast, the homogeneous catalyst produces lower molecular weight polymer (M_n = 140 kg mol^{-1}) than **1** (M_n = 533.7 kg mol^{-1}). GPC analysis shows that **1** also produces a small amount of low molecular weight polymer (M_n = 13.9 kg mol^{-1}). Both the high molecular weight and low molecular weight fractions have narrow dispersity ($Đ$ = 1.7 and 1.2, respectively).

Increasing the polymerization temperature to 40 °C results in higher activity and higher molecular weight polymer while maintaining a narrow molecular weight distribution (Table 1, Entry 2).[25] Above this temperature activities and molecular weight of the polymers tend to decrease (Entries 3-5). Polymerization reactions in toluene show slightly lower activity than those in cyclohexane (Entry 6-7). In all cases, GPC analysis of the polymers show similar bimodal molecular weight distributions, with the high molecular weight fraction being dominant. Both fractions are characterized by narrow dispersity values ($Đ$ < 2).

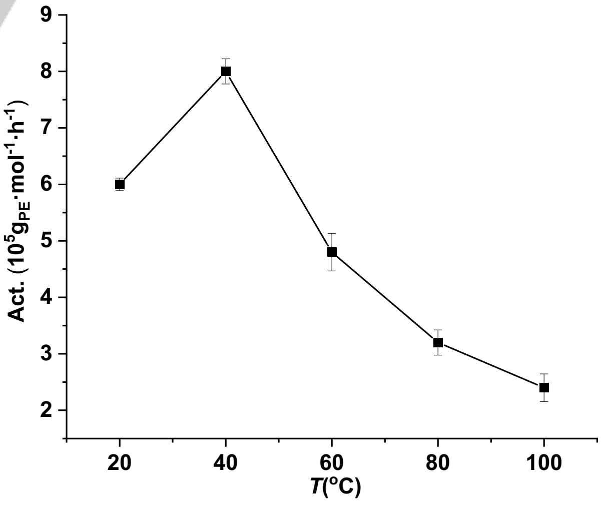

Figure 5. Activity of **1** in ethylene polymerization reactions. Each point is the average of at least three runs, and the error bars give the range of values obtained in these runs.

Table 1. Polymerization of ethylene and copolymerization of ethylene and methyl acrylate using **1**.[a]

Entry	*T (°C)*	*Solvent*	*Yield (g)*	*Act*[b]	*X (%)*[c]	*B*[d]	*M_n*[e]	*Đ*
1	20	C_6H_{12}	0.15	6.0	-	26	534 13.9	1.7 1.2
2	40	C_6H_{12}	0.20	8.0	-	27	972 14.0	1.6
3	60	C_6H_{12}	0.12	4.8	-	29	721 4.3	1.3
4	80	C_6H_{12}	0.08	3.2	-	32	341 9.1	1.3
5	100	C_6H_{12}	0.06	2.4	-	32	557 11.6	1.7
6	40	Toluene	0.16	6.4	-	29	928 9.3	1.7
7	60	Toluene	0.10	4.0	-	29	290 12.9	1.5
8[f]	40	C_6H_{12}	0.042	0.014	0.4	31	337 12.6	1.8
9[f]	60	C_6H_{12}	0.038	0.013	0.4	37	168 12.1	2.2
10[f]	40	Toluene	0.033	0.011	0.4	32	460 12.1	1.9
11[f]	60	Toluene	0.028	0.009	0.4	33	248.0	1.5

[a]Polymerization conditions: Pd catalyst = 0.5 μmol; solvent =5 mL, ethylene = 150 psi; reaction time = 0.5h. [b]Yields and activities are averages of at least three runs. Activity reported in 10^5 $g_{PE}\cdot mol^{-1}\cdot h^{-1}$. [c] Incorporation of methyl acrylate into the co-polymer determined by ^1H NMR in tetrachloroethane-d_2 at 120 °C. [d]Number of branches per 1000 carbons determined by ^1H NMR in tetrachloroethane-d_2 at 120 °C. [e] Reported in kg/mol. Determined by GPC in trichlorobenzene at 140 °C. [f]2 μmol Pd catalyst, MA added as a 1 M solution in the listed solvent, ethylene = 80 psi; reaction time = 15h.

Images form scanning electron mircroscopy (SEM) of the polyethylene produced by **1** or solutions of (N^N)Pd(CH_3)Cl activated with Na[B(Ar^F)$_4$] are shown in Figure SX. At 40 °C, **1** produces polymers that are small, precipitated pellets commonly produced by heterogeneous polymerization catalysts. In contrast, the solution catalyst forms a large globular mass suspended in reaction solvent (Figure S21). SEM images show that all polymers produced by **1** at 20 ºC to 60 ºC have particulate morphologies of approximately 400 μM in size, similar to the morphology of **1** from SEM imaging. This defined morphology is lost when polymerizations are performed at 80 °C or 100 °C (Figure S21). No discernable morphology is obtained for the polymer prepared with solutions of (N^N)Pd(CH_3)Cl and Na[B($Ar^F$$_4$)] (Figure S21).

Table 1 also includes data for the copolymerization of ethylene and methyl acrylate catalyzed by **1** (Entries 8 – 11). The activity of **1** decreases by roughly two orders of magnitude in copolymerization reactions of ethylene and methyl acrylate (eq 3, Table 1, Entries 8-11). This behavior is typical of copolymerization reactions catalyzed by (N^N)Pd–Me^+ catalysts. Similar to ethylene polymerization reactions, higher temperatures decrease the molecular weight of the copolymer, and similar polymers are isolated from cyclohexane or toluene.

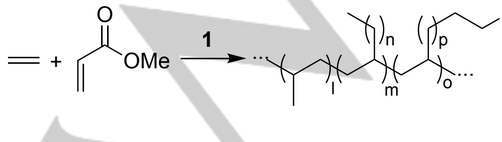

(3)

SEM imaging of the copolymers show comparable morphologies as polyethylenes generated by **1** (Figure S19). The ^1H NMR spectra of the copolymers in $C_2D_2Cl_4$ at 120 °C shows that **1** incorporates 0.4 % methylacrylate at the chain ends, similar to (N^N)Pd(CH_3)Cl activated with Na[B(Ar^F)$_4$] in solution.[17b] GPC analysis of the copolymers again shows bimodal, narrow molecular weight distributions of polymer. However, the high molecular weight fraction produced by **1** is significantly higher than produced by solutions of (N^N)Pd(CH_3)Cl activated with Na[B(Ar^F)$_4$].

The bimodal polymer composition complicates conclusions about the ability of **1** to incorporate methyl acrylate into high molecular weight polymers. A plausible scenario is methyl acrylate inserts into Pd–R^+, followed by chain-walking and chain-transfer to yield the low molecular weight fraction. This behavior is common in (α-diimine)Pd–R^+ copolymerization of ethylene and methylacrylate.[6c] In this scenario the high molecular weight fraction would form by polymerization of ethylene, and would not contain methyl acrylate at the chain ends. Partial fractionation of the copolymer produced by **1** (Table 1, Entry 8) separates out the highest molecular weight polymer products (M_n = 1437.4 kg mol^{-1}; $Đ$ = 1.2). ^1H NMR analysis of this high molecular weight fraction in $C_2D_2Cl_4$ at 120 °C shows that 0.5 % methylacrylate incorporation at the chain ends, indicating that **1** does indeed incorporate methyl acrylate into the high molecular weight polymer fraction (Figure S15-S18). This copolymer produced by **1** is higher molecular weight than other (α-diimine)Pd–R^+ catalysts, and is also higher than electron-rich Pd-cations that incorporate acrylates into the polymer chain.[26]

The lowest molecular weight fraction (M_n = 98.4 kg mol^{-1}) obtained from partial fractionation experiments also contains 0.4 % methylacrylate. In addition, the ^1H NMR spectrum of the low molecular weight fraction in $C_2D_2Cl_4$ at 120 °C contains signals for internal olefins (Figure S36), which is consistent with chain-transfer by β-hydride elimination that is common in (N^N)Pd–Me^+ catalysts.

Abstraction of halides from precatalysts is by far the most common method to generate catalytically active ion-pairs

10.1002/anie.202117279

containing weakly coordinating anions in solution.[27] Similar methods were not broadly available for reactions that functionalize surfaces. The R_3Si^+ mediated halide abstraction from $(N^\wedge N)Pd(CH_3)Cl$ to form **1** fills this methodological gap left from the more common reactions of organometallics with acidic –OH groups on partially dehydroxylated oxides[28] or with the strong Lewis sites present on partially dehydroxylated aluminas[29] or silica-aluminas.[30] $[^iPr_3Si][(R^FO)_3Al–OSi\equiv)]$ contains ~1 $^iPr_3Si^+$ nm^{-2}, suggesting that high surface coverage of ion-pairs may be accessible using this halide abstraction methodology with sterically small metal halide reagents. An important observation in the reaction of $(N^\wedge N)Pd(CH_3)Cl$ and $[^iPr_3Si][(R^FO)_3Al–OSi\equiv)]$ is only **1** and $^iPr_3Si–Cl$ form. One may expect that **2** and $^iPr_3Si–Me$ would also form in this reaction, but silylium ions have some of the highest reported halide ion affinities,[15] a manifestation of their strong Lewis acidity and the driving force for selective formation of **1** and $^iPr_3Si–Cl$ instead of **2** and $^iPr_3Si–Me$.

1 shows distinct reactivity compared to $[(N^\wedge N)Pd–CH_3]^+$ supported on sulfated zirconium oxide. First, in the latter case only ~9 % of Pd sites are active in ethylene polymerization. Virtually all $Pd–CH_3^+$ sites in **1** insert vinyl chloride to form propene and **2**, and also follow similar reactivity patterns as other $(\alpha\text{-diimine})Pd–R^+$ with vinyl chloride.[21b] Active site counts approaching 100% are rare in heterogeneous catalysts for olefin polymerization.[31] Second, **1** produces polymers with significantly higher molecular weights than $[(N^\wedge N)Pd–CH_3]^+$ supported on sulfated zirconium oxide or solutions of $(N^\wedge N)Pd(CH_3)Cl$ activated with $Na[B(Ar^F)_4]$.

These reactivity patterns indicate that the support effects in **1** promote active site formation and suppress chain transfer processes. $^{13}C\{^{27}Al\}$ PM-RESPDOR and $^1H\{^{19}F\}$ S-REDOR experiments show that the Pd–Al distance between $[(N^\wedge N)Pd–CH_3]^+$ and $[(R^FO)_3Al–OSi\equiv)]$ is 11 Å, consistent with a weakly coordinated ion-pair in **1**. The coordination of a nearby ≡Si–O–Si≡ bridge to the $[(N^\wedge N)Pd–CH_3]^+$ fragment, common in organometallics supported on silica,[20] results in a similar coordination environment at Pd as the classic $(\alpha\text{-diimne})Pd(CH_3)(Et_2O)^+$ that reacts with ethylene by associative ligand exchange to form $(\alpha\text{-diimne})Pd(CH_3)(H_2C{=}CH_2)^+$ and Et_2O.[32] Associative displacement of the coordinated ≡Si–O–Si≡ bridge in **1** by ethylene is expected to form the active alkyl-ethylene intermediate shown in Figure 7. Indeed, DFT studies of $[Cp_2Zr–CH_3][H_3C–AlOx]$, formed by the reaction of $Cp_2Zr(CH_3)_2$ with fully dehydrated alumina, showed that the metallocenium coordinates to nearby framework alumina sites (*i.e.* ≡Al–O–Al≡ bridges) far from the $[H_3C–AlOx]$ anion, and that the calculated energy required to displace ≡Al–O–Al≡ bridges by ethylene to form the alkyl-ethylene intermediate is less than a typical $[MeB(C_6F_5)_3]$ weakly coordinating anion.[33]

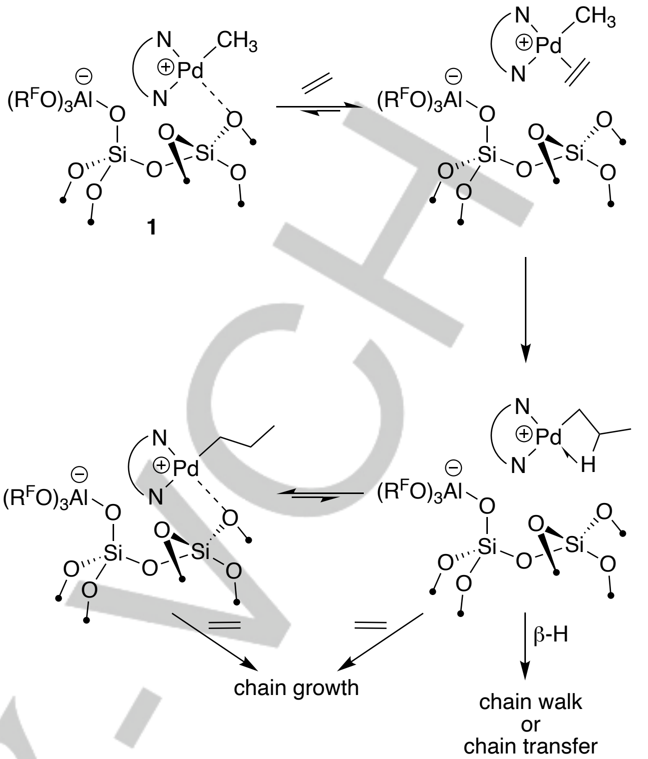

Figure 7. Proposed behavior of **1** consistent with experimental results.

Chain transfer in $[(\alpha\text{-diimine})Pd\text{-}CH_3]^+$ occurs through β-hydride elimination followed by associative ligand exchange with free ethylene.[6c] The sterically large $(N^\wedge N)$ ligand in **1** inhibits the formation of the β-agostic intermediate that precedes β-hydride elimination.[34] The fact that **1** produces significantly higher molecular weight polymer than solutions of $(N^\wedge N)Pd(CH_3)Cl$ and $Na[B(C_6F_5)_4]$ suggests that coordination of a ≡Si–O–Si≡ bridge further inhibits the formation of the β-agostic intermediate and suppresses chain transfer, Figure 7.

The narrow molecular weight distributions of polymers produced by **1** are in contrast to more typical heterogeneous compositions containing $(\alpha\text{-diimine})NiBr_2/Et_3Al_2Cl_3/[AlMe_3/SiO_2]$.7 However, why **1** produces a bimodal molecular weight distribution is somewhat less clear. This behavior could be related to the heterogeneity of the silica surface,[20f, 35] or subtle differences in ion-pairing that are known to affect activity in cationic Pd catalysts for polymerization reactions.[36] Evidently some of these environments prevents polymer growth, but the narrow dispersity of both the high and low molecular weight fractions indicates that all $Pd–Me^+$ sites are in well-defined coordination environments. This behavior is unusual, but not without precedent. For example, $Zr–R^+$ sites embedded in the pores of metal organic frameworks (MOFs) produce low molecular weight polymers while $Zr–R^+$ sites on the MOF surface produce high molecular weight polymer, both of which have narrow molecular weight properties indicative of well-defined coordination environements for the $Zr–R^+$ fragments.[37]

Conclusion

The reaction of $[^iPr_3Si][(R^FO)_3Al–OSi\equiv)]$ and $(N^\wedge N)Pd(CH_3)Cl$ abstracts a chloride from Pd to generate well-defined $[(N^\wedge N)Pd(CH_3)][(R^FO)_3Al–OSi\equiv)]$, which is active in olefin (co)polymerization reactions. Vinyl chloride titration experiments show that all $Pd–Me^+$ sites in this material are active in olefin insertion reactions. This is a drastic improvement from previous results showing that only ~9% of the $Pd–Me^+$ were active in olefin polymerization using catalysts generated from (α-diimine)Pd(CH_3)$_2$ and Bronsted acidic –OH sites on sulfated zirconium oxide.[12] The ability of $[^i\mathrm{Pr_3Si}][(\mathrm{R^FO})_3\mathrm{Al{-}OSi}\equiv)]$ to abstract halides from (N^N)Pd(CH_3)Cl to form **1** introduces a new synthetic strategy to form ion-pairs on surfaces that is complementary to known methods. Silylium-like ions have very high chloride ion affinities, suggesting that $[^i\mathrm{Pr_3Si}][(\mathrm{R^FO})_3\mathrm{Al{-}OSi}\equiv)]$ may be a general heterogeneous reagent for halide abstraction reactions. We are currently investigating this possibility.

Acknowledgements

M. P. C. is a member of the UCR Center for Catalysis. This work was led by the National Science Foundation (CHE-2101582). Solid-state NMR work was supported in part by the National Science Foundation under Grant No. CBET-1916809 (R.W.D and A.J.R) and the U.S. Department of Energy (DOE), Office of Basic Energy Sciences, Division of Chemical Sciences, Geosciences, and Biosciences (G.P.L and F.A.P). Ames Laboratory is operated for the DOE by Iowa State University under Contract No. DE-AC02-07CH11358. A.J.R. acknowledges additional support from the Alfred P. Sloan Foundation through a Sloan research fellowship.

Keywords:; Palladium • Olefin Polymerization • Polar Monomer • Heterogeneous Catalysis • Solid- state NMR

[1] a) G. G. Hlatky, *Chem. Rev.* **2000**, *100*, 1347-1376; b) J. R. Severn, J. C. Chadwick, R. Duchateau, N. Friederichs, *Chem. Rev.* **2005**, *105*, 4073-4147; c) M. Stürzel, S. Mihan, R. Mülhaupt, *Chemical Reviews* **2016**, *116*, 1398-1433.
[2] M. Bochmann, *Organometallics* **2010**, *29*, 4711-4740.
[3] W. Kaminsky, *Dalton Trans.* **1998**, 1413-1418.
[4] J. C. Chadwick, T. Garroff, J. R. Severn, in *Tailor-Made Polymers*, **2008**, pp. 43-78.
[5] D. B. Culver, R. W. Dorn, A. Venkatesh, J. Meeprasert, A. J. Rossini, E. A. Pidko, A. S. Lipton, G. R. Lief, M. P. Conley, *ACS Cent. Sci.* **2021**, *7*, 1225-1231.
[6] a) C. Tan, C. Chen, *Angew. Chem., Int. Ed.* **2019**, *58*, 7192-7200; *Angew. Chem.* **2019**, *131*, 7268-7276; b) C. Chen, *Nat. Rev. Chem.* **2018**, *2*, 6-14; c) S. D. Ittel, L. K. Johnson, M. Brookhart, *Chem. Rev.* **2000**, *100*, 1169-1204; d) A. Nakamura, T. M. J. Anselment, J. Claverie, B. Goodall, R. F. Jordan, S. Mecking, B. Rieger, A. Sen, P. W. N. M. van Leeuwen, K. Nozaki, *Acc. Chem. Res.* **2013**, *46*, 1438-1449; e) A. Nakamura, S. Ito, K. Nozaki, *Chem. Rev.* **2009**, *109*, 5215-5244.
[7] a) P. Preishuber-Pflugl, M. Brookhart, *Macromolecules* **2002**, *35*, 6074-6076; b) H. S. Schrekker, V. Kotov, P. Preishuber-Pflugl, P. White, M. Brookhart, *Macromolecules* **2006**, *39*, 6341-6354; c) J. R. Severn, J. C. Chadwick, V. Van Axel Castelli, *Macromolecules* **2004**, *37*, 6258-6259.
[8] S. Tsuji, D. C. Swenson, R. F. Jordan, *Organometallics* **1999**, *18*, 4758-4764.
[9] P. Wucher, J. B. Schwaderer, S. Mecking, *ACS Catal.* **2014**, *4*, 2672-2679.
[10] H. Zhang, C. Zou, H. Zhao, Z. Cai, C. Chen, *Angew. Chem., Int. Ed.* **2021**, *60*, 17446-17451; *Angew. Chem.* **2021**, *133*, 17586-17591.
[11] R. J. Witzke, A. Chapovetsky, M. P. Conley, D. M. Kaphan, M. Delferro, *ACS Catal.* **2020**, 11822-11840.
[12] D. B. Culver, H. Tafazolian, M. P. Conley, *Organometallics* **2018**, *37*, 1001-1006.
[13] a) Y.-J. Wanglee, J. Hu, R. E. White, M.-Y. Lee, S. M. Stewart, P. Perrotin, S. L. Scott, *J. Am. Chem. Soc.* **2012**, *134*, 355-366; b) J. F. Walzer, **1995**; cN. Millot, C. C. Santini, A. Baudouin, J.-M. Basset, *Chem. Commun.* **2003**, 2034-2035.
[14] a) D. B. Culver, A. Venkatesh, W. Huynh, A. J. Rossini, M. P. Conley, *Chem. Sci.* **2020**, *11*, 1510 - 1517; b) D. B. Culver, M. P. Conley, *Angew. Chem., Int. Ed.* **2018**, *57*, 14902-14905; ; *Angew. Chem.* **2018**, *130*, 15118-15121.
[15] H. F. T. Klare, L. Albers, L. Süsse, S. Keess, T. Müller, M. Oestreich, *Chem. Rev.* **2021**, *121*, 5889-5985.
[16] a) C. Douvris, C. A. Reed, *Organometallics* **2008**, *27*, 807-810; b) F.-S. Guo, Y.-C. Chen, M.-L. Tong, A. Mansikkamäki, R. A. Layfield, *Angew. Chem., Int. Ed.* **2019**, *58*, 10163-10167; *Angew. Chem.* **132**, 2319-2323; c) F.-S. Guo, B. M. Day, Y.-C. Chen, M.-L. Tong, A. Mansikkamäki, R. A. Layfield, *Science* **2018**, *362*, 1400-1403; d) C. A. P. Goodwin, D. Reta, F. Ortu, N. F. Chilton, D. P. Mills, *J. Am. Chem. Soc.* **2017**, *139*, 18714-18724; e) H. M. Nicholas, M. Vonci, C. A. P. Goodwin, S. W. Loo, S. R. Murphy, D. Cassim, R. E. P. Winpenny, E. J. L. McInnes, N. F. Chilton, D. P. Mills, *Chem. Sci.* **2019**, *10*, 10493-10502; f) C. A. P. Goodwin, F. Ortu, D. Reta, N. F. Chilton, D. P. Mills, *Nature* **2017**, *548*, 439-442; g) F.-S. Guo, B. M. Day, Y.-C. Chen, M.-L. Tong, A. Mansikkamäki, R. A. Layfield, *Angew. Chem., Int. Ed.* **2017**, *56*, 11445-11449; hV. Varga, M. Lamač, M. Horáček, R. Gyepes, J. Pinkas, *Dalton Trans.* **2016**, *45*, 10146-10150.
[17] a) J. L. Rhinehart, L. A. Brown, B. K. Long, *J. Am. Chem. Soc.* **2013**, *135*, 16316-16319; b) S. Dai, X. Sui, C. Chen, *Angew. Chem., Int. Ed.* **2015**, *54*, 9948-9953; *Angew. Chem.* **2015**, *127*, 10086-10091; c) S. Dai, C. Chen, *Angew. Chem. Int.Ed.* **2016**, *55*, 13281-13285; *Angew. Chem.* **2016**, *128*, 13475-13479.
[18] a) Z. Gan, *Chem. Commun.* **2006**, 4712-4714; b) L. Chen, Q. Wang, B. Hu, O. Lafon, J. Trébosc, F. Deng, J.-P. Amoureux, *Phys. Chem. Chem. Phys.* **2010**, *12*, 9395-9405; c) E. Nimerovsky, R. Gupta, J. Yehl, M. Li, T. Polenova, A. Goldbourt, *J. Magn. Reson.* **2014**, *244*, 107-113.
[19] A. Brinkmann, A. P. M. Kentgens, *J. Am. Chem. Soc.* **2006**, *128*, 14758-14759.
[20] a) E. Le Roux, M. Chabanas, A. Baudouin, A. de Mallmann, C. Copéret, E. A. Quadrelli, J. Thivolle-Cazat, J.-M. Basset, W. Lukens, A. Lesage, L. Emsley, G. J. Sunley, *J. Am. Chem. Soc.* **2004**, *126*, 13391-13399; b) B. Rhers, A. Salameh, A. Baudouin, E. A. Quadrelli, M. Taoufik, C. Copéret, F. Lefebvre, J.-M. Basset, X. Solans-Monfort, O. Eisenstein, W. W. Lukens, L. P. H. Lopez, A. Sinha, R. R. Schrock, *Organometallics* **2006**, *25*, 3554-3557; c) M. P. Conley, G. Lapadula, K. Sanders, D. Gajan, A. Lesage, I. del Rosal, L. Maron, W. W. Lukens, C. Copéret, R. A. Andersen, *J. Am. Chem. Soc.* **2016**, *138*, 3831-3843; d) M. Chabanas, A. Baudouin, C. Coperet, J.-M. Basset, W. Lukens, A. Lesage, S. Hediger, L. Emsley, *J. Am. Chem. Soc.* **2002**, *125*, 492-504; e) E. Mazoyer, N. Merle, A. d. Mallmann, J.-M. Basset, E. Berrier, L. Delevoye, J.-F. Paul, C. P. Nicholas, R. M. Gauvin, M. Taoufik, *Chem. Commun.* **2010**, *46*, 8944-8946; f) D. B. Culver, W. Huynh, H. Tafazolian, M. P. Conley, *Organometallics* **2020**, *39*, 1112-1122; g) N. Merle, J. Trebosc, A. Baudouin, I. D. Rosal, L. Maron, K. Szeto, M. Genelot, A. Mortreux, M. Taoufik, L. Delevoye, R. g. M. Gauvin, *J. Am. Chem. Soc.* **2012**, *134*, 9263-9275.
[21] a) S. R. Foley, R. A. Stockland, H. Shen, R. F. Jordan, *J. Am. Chem. Soc.* **2003**, *125*, 4350-4361; b) S. M. Kilyanek, E. J. Stoebenau, N. Vinayavekhin, R. F. Jordan, *Organometallics* **2010**, *29*, 1750-1760.
[22] a) Z. Liu, E. Somsook, C. R. Landis, *J. Am. Chem. Soc.* **2001**, *123*, 2915-2916; b) D. L. Nelsen, B. J. Anding, J. L. Sawicki, M. D. Christianson, D. J. Arriola, C. R. Landis, *ACS Catal.* **2016**, *6*, 7398-7408; c) Y. Yu, R. Cipullo, C. Boisson, *ACS Catal.* **2019**, *9*, 3098-3103; d) I. Guerrero-Ríos, E. Novarino, B. Hessen, M. W. Bouwkamp, *Organometallics* **2015**, *34*, 5589-5596.
[23] D. M. Philipp, R. P. Muller, W. A. Goddard, J. Storer, M. McAdon, M. Mullins, *J. Am. Chem. Soc.* **2002**, *124*, 10198-10210.
[24] M. Pérez, L. J. Hounjet, C. B. Caputo, R. Dobrovetsky, D. W. Stephan, *J. Am. Chem. Soc.* **2013**, *135*, 18308-18310.
[25] Pd-catalysts for olefin polymerization usually have lower activity as the reaction temperature increases. The origin of the behavior shown in Figure 6 is not clear. However, similar behavior was

observed for solutions of (N^N)Pd(CH_3)Cl and Na[B(Ar^F_4)], see ref 17b for details.

[26] W. Zhang, P. M. Waddell, M. A. Tiedemann, C. E. Padilla, J. Mei, L. Chen, B. P. Carrow, *J. Am. Chem. Soc.* **2018**, *140*, 8841-8850.

[27] a) I. M. Riddlestone, A. Kraft, J. Schaefer, I. Krossing, *Angew. Chem., Int. Ed.* **2018**, *57*, 13982-14024; *Angew. Chem.* **2008**, *120*, 7772-7776; b) A. Macchioni, *Chem. Rev.* **2005**, *105*, 2039-2074.

[28] a) C. Copéret, A. Comas-Vives, M. P. Conley, D. P. Estes, A. Fedorov, V. Mougel, H. Nagae, F. Núñez-Zarur, P. A. Zhizhko, *Chem. Rev.* **2016**, *116*, 323-421; b) S. L. Wegener, T. J. Marks, P. C. Stair, *Acc. Chem. Res.* **2011**, *45*, 206-214; c) J. D. A. Pelletier, J.-M. Basset, *Acc. Chem. Res.* **2016**, *49*, 664-677.

[29] P. J. Toscano, T. J. Marks, *J. Am. Chem. Soc.* **1985**, *107*, 653-659.

[30] M. Jezequel, V. Dufaud, M. J. Ruiz-Garcia, F. Carrillo-Hermosilla, U. Neugebauer, G. P. Niccolai, F. Lefebvre, F. Bayard, J. Corker, S. Fiddy, J. Evans, J.-P. Broyer, J. Malinge, J.-M. Basset, *J. Am. Chem. Soc.* **2001**, *123*, 3520-3540.

[31] a) C. P. Nicholas, H. Ahn, T. J. Marks, *J. Am. Chem. Soc.* **2003**, *125*, 4325-4331; b) L. A. Williams, N. Guo, A. Motta, M. Delferro, I. L. Fragala, J. T. Miller, T. J. Marks, *Proc. Nat. Acad. Sci. USA* **2013**, *110*, 413-418; c) H. Tafazolian, D. B. Culver, M. P. Conley, *Organometallics* **2017**, *36*, 2385-2388.

[32] D. J. Tempel, L. K. Johnson, R. L. Huff, P. S. White, M. Brookhart, *J. Am. Chem. Soc.* **2000**, *122*, 6686-6700.

[33] A. Motta, I. L. Fragalà, T. J. Marks, *J. Am. Chem. Soc.* **2008**, *130*, 16533-16546.

[34] L. Guo, S. Dai, X. Sui, C. Chen, *ACS Catal.* **2016**, *6*, 428-441.

[35] D. Gajan, C. Coperet, *New J. Chem.* **2011**, *35*, 2403-2408.

[36] B. Binotti, G. Bellachioma, G. Cardaci, C. Carfagna, C. Zuccaccia, A. Macchioni, *Chemistry – A European Journal* **2007**, *13*, 1570-1582.

[37] R. C. Klet, S. Tussupbayev, J. Borycz, J. R. Gallagher, M. M. Stalzer, J. T. Miller, L. Gagliardi, J. T. Hupp, T. J. Marks, C. J. Cramer, M. Delferro, O. K. Farha, *J. Am. Chem. Soc.* **2015**, *137*, 15680-15683.

Entry for the Table of Contents

Insert graphic for Table of Contents here.

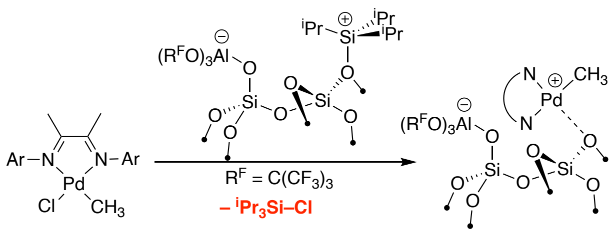

R_3Si^+ Mediated Halide Abstraction on Activated Silica

A silylium-like ion supported on silica ionizes a Pd–Cl complex by chloride abstraction to generate a very active catalyst for (co-)polymerization reactions.